Evaluation of Therapy Response in Children with Untreated Malignant Lymphomas Using Technetium-99m-Sestamibi

L. Özlem Kapucu, Canan Akyüz, Gülin Vural, Aynur Oguz, Tamer Atasever, Münevver Büyükpamukçu and Mustafa Ünlü
Departments of Nuclear Medicine and Pediatric Oncology, Faculty of Medicine, Gazi University; and Department of Pediatric Oncology, Hacettepe University, Ankara, Turkey

The aim of this study was to investigate the relationship between ^{99m}Tc-sestamibi accumulation in tumors and response to chemotherapy in children with untreated malignant lymphomas. **Methods:** Twenty-four children with malignant lymphoma (16 with Hodgkin's disease and 8 with non-Hodgkin's lymphoma) were studied with ^{201}Tl and then with ^{99m}Tc-sestamibi scintigraphy before any therapeutic intervention. Visual and quantitative interpretation of ^{201}Tl and ^{99m}Tc-sestamibi scans were performed. Visual uptake scores ≥2+ were considered positive studies for ^{201}Tl and ^{99m}Tc-sestamibi scintigraphy. Remission rates were evaluated at the end of induction therapy; patients were then followed clinically for 1–2 yr. **Results:** All 17 patients who had positive ^{99m}Tc-sestamibi scans subsequently had a complete response to chemotherapy; all seven patients who had negative ^{99m}Tc-sestamibi scans subsequently had partial or no response to chemotherapy, irrespective of the lymphoma type. The mean tumor-to-background ratios of patients with complete response and with partial or no response were 1.395 ± 0.2 and 1.031 ± 0.05 ($p = 0.0002$), respectively. Thallium-201 scintigraphy results were not related to the response to chemotherapy. **Conclusion:** Technetium-99m-sestamibi scintigraphy can provide information predicting the response to chemotherapy in patients with malignant lymphoma.

Key Words: lymphoma; thallium-201; technetium-99m-sestamibi; chemotherapy response

J Nucl Med 1997; 38:243–247

Lymphomas constitute approximately 10% of all childhood cancers, being third in relative frequency after acute leukemias and brain tumors. The primary therapeutic modality for all histologies and stages of childhood non-Hodgkin's lymphoma is chemotheraphy (*1*) and chemotherapy and radiotherapy for Hodgkin's disease (*2*).

Resistance of malignant tumors to chemotherapeutic agents is a major cause of treatment failure. Multidrug resistance (MDR) is a term that describes the phenomenon by which a cancer either intrinsically or in response to prior therapy becomes resistant to multiple drugs that have little similarity in their chemical structure and mechanism of action (*3,4*). It is associated with P-glycoprotein (Pgp) overexpression in tumor cells, an energy-dependent drug efflux pump, encoded by the MDR1 gene (*5*). Pgp recognizes and transports a large group of cytotoxic compounds including the anthracyclines, vinca alkoloids, epipodophyllotoxins, colchicine and actinomycin D (*6,7*), which share little or no structural or functional similarities (*8,9*), other than being relatively small, hydrophobic and cationic (*10*).

Pgp overexpression has been associated with clinical evidence of drug resistance and treatment failure (*11*). It has been suggested that determinations of Pgp glycoprotein levels in patients at diagnosis or relapse may have a major role in the design of future treatment protocols (*12*).

Recent studies have demonstrated that hexakis (2-methoxyisobutyl isonitrile) technetium (^{99m}Tc-sestamibi), a lipophilic cationic radiopharmaceutical useful in myocardical perfusion imaging, has lower accumulation in Pgp-enriched hamster cell lines compared to their respective parental drug-sensitive cell lines (*13*), and ^{99m}Tc-sestamibi is a transport substrate recognized by the human MDR1 Pgp (*14*). These findings suggest that ^{99m}Tc-sestamibi may prove useful for functionally characterizing Pgp expression, and MDR, in human tumors in vivo.

The aim of this study was to clinically investigate the relation between ^{99m}Tc-sestamibi accumulation in tumors and response to chemotherapy and clinical outcome in children with untreated malignant lymphomas.

MATERIALS AND METHODS

Patients

A consecutive series of 24 children (13 boys, 11 girls; age range 1–17 yr; mean age 9.5 ± 4.4 yr) with untreated malignant lymphoma (16 with Hodgkin's disease and 8 with non-Hodgkin's lymphoma) were studied first with ^{201}Tl and then ^{99m}Tc-sestamibi scintigraphy before any therapeutic intervention (Table 1). Only supradiaphragmatic lesions were evaluated in the study because visualization of lesions located in intra-abdominal and inguinal regions were unreliable due to the physiological tracer accumulation in intra-abdominal organs.

The extent of disease at diagnosis was categorized according to the Ann Arbor (*2*) staging system for Hodgkin's disease (HD) and St. Jude (*1*) staging system for non-Hodgkin's lymphoma (NHL). Informed consent from each patient's parents was supplied.

After the imaging study, all patients received multiagent chemotherapy according to their lymphoma type and clinical stage, and radiotherapy was added to the regimen in 14 patients with HD and in 2 patients with NHL (Table 1). Multiagent chemotherapy for patients with HD was scheduled according to the ABVD and/or MOPP protocols (*2*). Patients with NHL were treated with the LSA_2L_2 and/or BFM protocols (*1*).

Remission rates were evaluated at the end of the induction therapy. Positive response of the lesions to therapy, at the time of primary disease, were evaluated by clinical and radiological methods. Evaluation criteria were:

1. Complete response (CR) = no evidence of disease.
2. Partial response (PR) = ≥50% decrease in the sum of the product of the maximum perpendicular diameters of all measurable lesions; no evidence of progression in any lesion and no new lesions.
3. No response (NR) = <25% increase in the sum of the product of the maximum perpendicular diameters of all

Received Feb. 22, 1996; revision accepted June 15, 1996.
For correspondence or reprints contact: L.Özlem Kapucu, Department of Nuclear Medicine, Gazi University, Hosdere Caddesi 3/17, Yukari Ayranci, 06540, Ankara, Turkey.

TABLE 1
Clinical and Scintigraphic Findings

Patient no.	Age	Sex	Tumor type	^{201}Tl	^{99m}Tc-sestamibi	Stage	Therapy	Response	Current status
1	13	M	HD	Positive	Positive	III	Che + RT	CR	NED
2	12	F	HD	Positive	Positive	IIB	Che + RT	CR	NED
3	14	F	HD	Positive	Positive	II	Che + RT	CR	NED
4	6	F	HD	Positive	Positive	II	Che + RT	CR	NED
5	10	M	HD	Positive	Positive	III	Che + RT	CR	NED
6	14	F	HD	Positive	Positive	II	Che + RT	CR	NED
7	17	M	HD	Positive	Positive	II	Che	CR	NED
8	12	F	HD	Positive	Positive	III	Che + RT	CR	NED
9	7	M	HD	Positive	Positive	III	Che + RT	CR	NED
10	5	M	HD	Positive	Positive	II	Che	CR	NED
11	8	F	HD	Positive	Positive	IIIA	Che + RT	CR	NED
12	11	M	HD	Positive	Positive	II	Che + RT	CR	NED
13	6	F	HD	Positive	Positive	IIIS	Che + RT	CR	NED
14	12	M	HD	Positive	Positive	III	Che + RT	CR	NED
15	14	F	HD	Positive	Negative	IV	Che + RT	PR	AliveWD
16	7	M	HD	Positive	Negative	IV	Che	NR	Died
17	15	M	NHL	Positive	Negative	III	Che	PR,	Died
18	4	M	NHL	Positive	Negative	III	Che + RT	NR	AliveWD
19	14	F	NHL	Positive	Positive	III	Chemo	CR	NED
20	5	F	NHL	Positive	Negative	IV	Che	PR	Died
21	7	M	NHL	Positive	Positive	III	Che	CR	NED
22	5	M	NHL	Positive	Negative	IV	Che	PR	AliveWD
23	5	M	NHL	Positive	Positive	III	Che + RT	CR	NED
24	1	M	NHL	Positive	Negative	III	Che	NR	Died

HD = Hodgkin's disease; NHL = non-Hodgkin lymphoma; Che = chemotherapy; RT = radiotherapy; CR = complete response; PR = partial response; NR = no response; NED = no evidence of disease; AliveWD = alive with disease.

measurable lesions, no evidence of progression in any lesion and no new lesions.

4. Progressive disease (PD) = ≥25% increase in the sum of the product of the maximum perpendicular diameters of all measurable lesions and/or the appearance of new lesions. Patients were then followed clinically for 1–2 yr (mean: 1.34 yr).

Imaging

Planar scintigraphy of the supradiaphragmatic regions were performed after intravenous injection 1–3 mci (37–111 MBq) ^{201}Tl. Early (20 min) and late (3 hr) images were obtained in the anterior projection, using a large field of view camera equipped with a low-energy, general-purpose collimator. A single 20% energy window set at 72 keV was used and a preset count of 100,000 counts was obtained for the early and late images. Technetium-99m-sestamibi scintigraphy was performed at least one day after the ^{201}Tl study 45–60 min after injection of 5–10 μci (185–370 MBq) ^{99m}Tc-sestamibi. Static images of the supradiaphragmatic regions were obtained in the anterior projection by using a large field of view camera equipped with a low-energy, general-purpose collimator. A single 20% energy window set at 140 keV was used and 100,000 counts were obtained from each static image.

Visual and Quantitative Interpretations

Visual and quantitative interpretation of ^{201}Tl and ^{99m}Tc-sestamibi images were performed. Two experienced physicians reviewed the images. Early and late ^{201}Tl images were similar in regard to the number of positively detected lesions. Therefore, only late ^{201}Tl images were used in the evaluation for simplicity and uniformity.

For visual interpretation, a five-point semiquantitative rating system was used to compare ^{201}Tl and ^{99m}Tc-sestamibi studies in which zero indicated activity within the lesion to be equivalent to the background within the axilla (no detectable lesion): 1+ = equivocal, 2+ = definite lesion activity >axillary soft-tissue background, 3+ = activity <heart and 4+ = activity ≥heart.

For quantitative assessment, tumor-to-background ratios (T/B) were obtained from ^{201}Tl and ^{99m}Tc-sestamibi images. Regions of interest (ROIs) were outlined in the lesion area (tumor) with abnormal activity and in the contralateral normal side (background) for the neck and axilla lesions. Background activity for mediastinal lesions was defined as any normal soft-tissue activity in the thorax. ROIs in ^{99m}Tc-sestamibi were drawn corresponding to the lesions visualized in ^{201}Tl scintigraphy.

Uptake ≥2+ was considered a positive study for ^{201}Tl and ^{99m}Tc-sestamibi scans. When the number of lesions visualized on the sestamibi scan was less than the number of lesions on the ^{201}Tl scan, at least one lesion with grade 2 visualization was required to classify sestamibi scan as positive.

Thallium-201 and ^{99m}Tc-sestamibi images were analyzed and compared with respect to patient and site sensitivity. To calculate site sensitivity in abnormal tissue, lesions or sites included in the physical examination and thoracic CT scan were compared with abnormal activities on the ^{201}Tl and ^{99m}Tc-sestamibi images. Lesion sites included the right and left cervical-supraclavicular region, right and left axilla and the mediastinum. Patient sensitivity for ^{201}Tl and ^{99m}Tc-sestamibi was defined as at least one positive lesion with a visual grading score of ≥2+.

Statistical Analysis

The Mann-Whitney U-test was used to determine differences in the distribution of mean values between the HD and NHL groups. Additionally, differences in the distribution of mean values between two other groups, thallium versus sestamibi, according to prognosis, were also assessed with the Mann-Whitney U-test.

RESULTS

All patients had at least one or more lesions located in supradiaphragmatic regions which were demonstrated by ^{201}Tl scintigraphy. Technetium-99m-sestamibi scintigraphy posi-

TABLE 2
Visual and Quantitative Interpretation of the Results

Patient no.	Total lesion number	^{201}Tl scintigraphy			^{99m}Tc-sestamibi scintigraphy		
		Detected lesion number	Visual score (range)	T/B ratio (range)	Detected lesion number	Visual score (range)	T/B ratio (range)
1	2	1	3+	1.40	1	2+	1.27
2	2	2	2+–3+	1.25–1.39	2	1+–2+	1.13–1.18
3	2	2	2+–2+	1.22–1.30	1	1+–2+	1.14–1.19
4	1	1	3+	1.33	1	3+	1.30
5	3	2	3+–4+	1.38–1.49	2	3+–4+	1.34–1.46
6	2	2	3+–3+	1.30–1.34	1	1+–2+	1.11–1.24
7	4	4	2+–3+	1.21–1.43	4	2+–4+	1.25–1.80
8	2	2	3+–4+	1.36–1.90	2	3+–4+	1.30–1.50
9	1	1	2+	1.25	1	2+	1.21
10	1	1	3+	1.30	1	3+	1.30
11	2	2	2+–3+	1.24–1.30	2	2+–3+	1.20–1.30
12	3	1	4+	1.40	1	3+	1.28
13	2	2	4+–4+	2.60–2.60	2	3+–4+	1.70–2.00
14	1	1	4+	1.43	1	3+	1.39
15	3	1	2+	1.17	0	0	1.0
16	5	4	2+–2+	1.24–1.24	0	0	1.0
17	4	3	3+–3+	1.36–1.42	0	1+–1+	1.11–1.15
18	2	2	2+–3+	1.18–1.34	0	0	1.0
19	5	2	3+–4+	1.40–1.60	2	3+–4+	1.39–1.60
20	2	1	3+	1.35	0	0	1.0
21	1	1	3+	1.47	1	2+	1.30
22	3	1	4+	2.0	0	1+	1.11
23	1	1	3+	1.4	1	3+	1.38
24	1	1	3+	1.50	0	1+	1.10
Total	55	41			27		

T/B = tumor-to-background.

tively detected at least one of these lesions in 14 of 16 patients with HD and in 3 of 8 patients with NHL, with an uptake score ≥2+ (Table 1). Patient sensitivity of ^{201}Tl and ^{99m}Tc-sestamibi was 100% and 70%, respectively.

Fifty-five lesion sites were detected by physical examination and CT, and 41 lesions were positive on ^{201}Tl scintigraphy (74%). On the other hand, 27 lesion sites were detected by ^{99m}Tc-sestamibi (49%) (Table 2). The smallest lesion detected by ^{201}Tl and ^{99m}Tc-sestamibi was 2.5 × 1 cm. Lesions scored as equivocal in ^{99m}Tc-sestamibi scintigraphy showed more prominent uptake in ^{201}Tl scintigraphy with at least 2+ visual uptake score (Table 2).

Thallium-201 accumulation in lesions were not related to lymphoma type (mean T/B ratios were 1.44 ± 0.4 and 1.40 ± 0.2 in HD and NHL lesions, respectively, $p > 0.05$) (Figs. 1, 2).Technetium-99m-sestamibi accumulation was greater in HD lesions than NHL (mean T/B ratio: 1.34 ± 0.2 versus 1.106 ± 0.2, $p = 0.005$) (Figs. 1, 2).

At the end of the induction therapy, partial or no response to chemotherapy leading to early relapse or death was observed in two patients with HD, one died, the other was alive with disease. In five patients with NHL, three died during follow-up and two had progressive disease with bone marrow involvement (Figs. 2, 3).

Patients who had complete response to chemotherapy had significantly different findings in ^{99m}Tc-sestamibi scintigraphy than patients who had partial or no response. All patients who had positive ^{99m}Tc-sestamibi scintigraphy subsequently had complete response to chemotherapy, and all patients who had negative ^{99m}Tc-sestamibi scintigraphy subsequently had partial or no response to chemotherapy, irrespective of the lymphoma type (Table 1). The mean ^{99m}Tc-sestamibi T/B ratios of patients with complete response and with partial or no response were 1.395 ± 0.2 and 1.031 ± 0.05 ($p = 0.0002$), respectively. The mean ^{99m}Tc-sestamibi/^{201}Tl ratios of patients with complete response and with partial or no response were 0.925 ± 0.14 and 0.752 ± 0.123 ($p = 0.009$), respectively.

We also compared some of the poor prognostic factors, including stage and histology with ^{99m}Tc-sestamibi accumulation in patients who had poor response to chemotherapy. While all 7 (100%) patients with poor prognosis had negative sestamibi results, 7 of 17 (41%) patients with an advanced stage (Stage III and IV) and 5 of 8 (63%) patients with NHL had poor prognoses (Table 1).

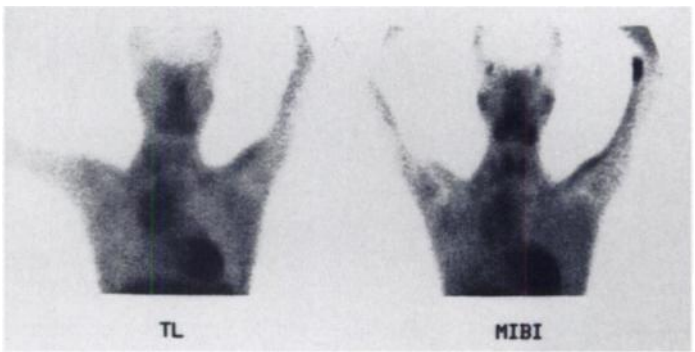

FIGURE 1. A 12-yr-old girl (Patient 8) with HD who had right cervical and mediastinal masses visualized by ^{201}Tl (left) and ^{99m}Tc-sestamibi scintigraphy (right). Visual grading scores and T/B ratios for cervical and mediastinal masses were 3+,1.36 and 4+, 1.90, respectively, in the ^{201}Tl study. They were 3+, 1.30 and 4+, 1.50, respectively, in the ^{99m}Tc-sestamibi study. The patient had complete response to subsequent chemotherapy.

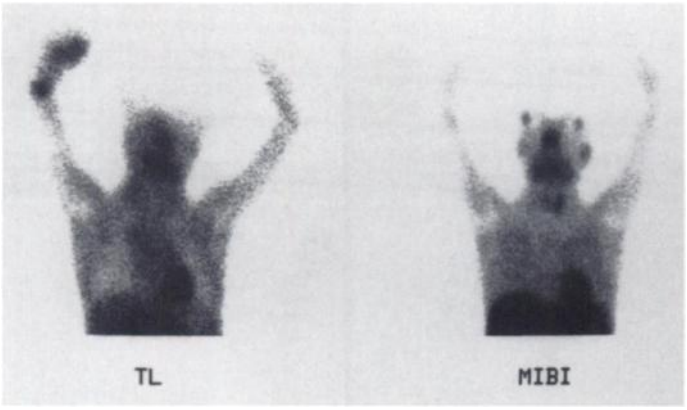

FIGURE 2. A 4-yr-old boy (Patient 18) with NHL, who had right cervical and mediastinal masses visualized by ^{201}Tl (left) scintigraphy. Technetium-99m-sestamibi (right) uptake was absent in these lesions. Visual grading scores and T/B ratios for cervical and mediastinal masses were 2+, 1.18 and 3+, 1.34, respectively, in the ^{201}Tl study. The patient demonstrated no response to subsequent chemotherapy.

The ^{201}Tl study was useful for scintigraphic visualization of the lesions, but ^{201}Tl scintigraphy results were not predictive for the response to subsequent chemotherapy.

DISCUSSION

General methods of detecting MDR1 expression in tissues include: assessing DNA amplification, measuring mRNA and quantitating the amount of Pgp. The multitude of assays and techniques used in clinical studies may produce various results for a given tumor type (*15*).

In a consecutive series of 42 patients with newly diagnosed malignant lymphomas, Miller et al. (*16*), using immunocytochemistry, found detectable levels of Pgp in only one patient. Goldstein et al. (*17*), using RNA slot blot methods, found Pgp in 4 of 18 previously untreated patients with lymphoma.

An important controversy in the field of MDR is whether identification of the expression of Pgp per se with antibodies or mRNA probes is sufficient, or is it necessary to assay directly the function of this transport protein (*14*). Given that regulatory pathways, such as protein kinase C-mediated phosphorylation (*8*) have been shown to modulate Pgp transport function, ^{99m}Tc-sestamibi may provide a unique opportunity to directly assay protein function in vivo and in vitro (*14*).

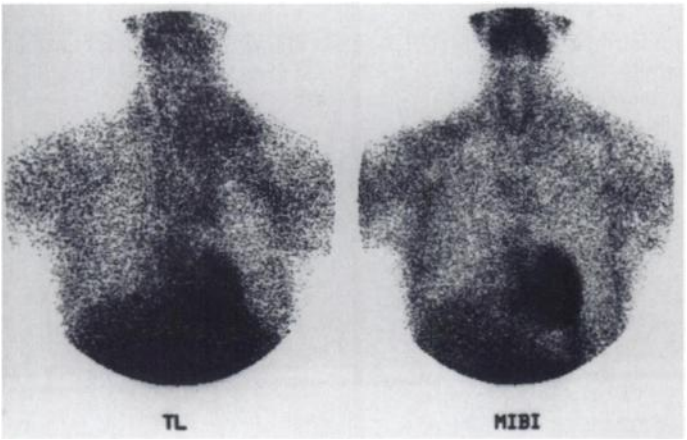

FIGURE 3. A 15-yr-old boy (Patient 17) with NHL, who had left cervical-supraclavicular and mediastinal masses visualized by ^{201}Tl (left) scintigraphy. Technetium-99m-sestamibi (right) accumulation in these lesions were faintly visualized. Visual grading scores and T/B ratios for cervical-supraclavicular and mediastinal masses were 3+, 1.36 and 3+, 1.42, respectively, in the ^{201}Tl study. They were 1+, 1.15 and 1+, 1.11, respectively, in the ^{99m}Tc-sestamibi study. The patient had partial response to subsequent chemotherapy but died.

In our study, a negative ^{99m}Tc-sestamibi scan—the inability to demonstrate lymphoma lesions with ^{99m}Tc-sestamibi when they were demonstrable by ^{201}Tl—indicated resistance to chemotherapy with partial or no response. On the other hand, patients who had lesions positively detected by ^{99m}Tc-sestamibi scintigraphy had complete remission and experienced no relapse during their 1–2-yr follow-up period. The overall rate of complete response to chemotherapy was significantly different in these two groups of patients with malignant lymphomas.

In view of the demonstrated role of Pgp in transporting both sestamibi molecules and chemotherapeutics outward from the tumor cells, we believe that the poor response to therapy in those patients with negative ^{99m}Tc-sestamibi scintigraphy was most probably related to overexpression or increased functioning of Pgp molecules. However, we cannot conclude this with certainty, since quantification of Pgp molecules with other conventional methods was not done.

During the last decade, neoplasms have become widely recognized as biologically heterogenous. At the time of diagnosis, most neoplasms consist of different populations of cells with diverse biologic characteristics (*18*). We may speculate that variable accumulation of ^{99m}Tc-sestamibi compared to ^{201}Tl may show, in part, the biological heterogeneity of tumor tissues as well.

Dimitrakopoulou-Strauss et al. (*19*) also studied tumor metabolism and MDR in patients with malignant lymphomas with FDG-PET and ^{99m}Tc-sestamibi. Their study differed from ours, in that the patients they evaluated had received chemotherapy before the scintigraphic evaluation. High uptake of ^{99m}Tc-sestamibi was observed in patients with stable disease or better. No sestamibi accumulation was observed in patients with progressive disease. The data support the hypothesis that sestamibi may reflect MDR (*19*). As they discussed in their study, while PET studies with FDG, before and after chemotherapy, are required to determine the effect of a cytostatic treatment, a single prechemotherapy study with ^{99m}Tc-sestamibi may be adequate for predicting therapeutic results. As in FDG-PET studies, ^{67}Ga and ^{201}Tl both need pre- and post-treatment scans for prognostic stratification in patients with malignant lymphomas and other tumors (*20–23*).

CONCLUSION

A single pretreatment scan with ^{99m}Tc-sestamibi may predict the clinical outcome and response to chemotherapy in patients with malignant lymphomas.

REFERENCES

1. Magrath I. Malignant non-Hodgkin's lymphomas in children. In: Pizzo PA, Poplack DG, eds. *Principles and practice of pediatric oncology,* 2nd ed. Philadelphia: J.B. Lippincott; 1993:537–575.
2. Leventhal BG, Donaldson SS. Hodgkin's disease. In: Pizzo PA, Poplack DG, eds. *Principles and practice of pediatric oncology,* 2nd ed. Philadelphia: J.B. Lippincott; 1993:577–594.
3. Pasten I, Gottesman M. Multiple-drug resistance in human cancer. *N Engl J Med* 1987;316:1388–1393.
4. Bradley G, Grunka PF, Ling V. Mechanisms of multidrug resistance. *Biochem Biophys Acta* 1988;948:87–128.
5. Endicott JA, Ling V. The biochemistry of P-glycoprotein-mediated multidrug resistance. *Ann Rev Biochem* 1989;58:137–171.
6. Gottesman MM, Patson I. The multidrug transporter: a double-edged sword. *J Biol Chem* 1988;263:12163–12166.
7. Fojo A, Akiyama S, Gottesman MM, et al. Reduced drug accumulation in multiple drug-resistant human KB carcinoma cell lines. *Cancer Res* 1985:3002–3007.
8. Ford JM, Hait WN. Pharmacology of drugs that alter multidrug resistance, MDR1, gene in neuroblastomas. *J Clin Oncol* 1990;8:128–136.
9. Ford JM, Bruggeman EP, Pasten I, Gottesman MM, Hait WN. Cellular and biochemical characterization of thioxanthenes for reversal of multidrug resistance in human and murine cell lines. *Cancer Res* 1990;50:1748–1756.
10. Pearce HI, Safa AR, Bach NJ, et al. Essential features of the P-glycoprotein

pharmacophore as defined by a series of reserpine analogs that modulate multidrug resistance. *Proc Natl Acad Sci USA* 1989;86:5128–5132.
11. Chan HLS, Haddad G, Thorner PS, et al. P-glycoprotein expression as a predictor of the outcome of therapy for neuroblastoma. *N Engl J Med* 1991;325:1608–1614.
12. Morrow CS, Cowan KH. Mechanisms of antineoplastic drug resistance. In: DeVita VT, Hellman S, Rosenberg SA, eds. *Cancer, principles and practice of oncology*, 4th ed. Philadelphia: J.B. Lippincott; 1993:340–348.
13. Piwnica-Worms D, Chiu ML, Budding M, et al. Functional imaging of multidrug-resistant P-glycoprotein with an organotechnetium complex. *Cancer Res* 1993;53:977–984.
14. Rao VV, Chiu ML, Kronauge JF, et al. Expression of recombinant human multidrug resistance P-glycoprotein in insect cells confers decreased accumulation of technetium-99m-sestamibi. *J Nucl Med* 1994;35:510–515.
15. Dalton WS. Overcoming the multidrug resistant phenotype. In: DeVita VT, Hellman S, Rosenberg SA, eds. *Cancer, principles and practice of oncology*, 4th ed. Philadelphia: J.B. Lippincott; 1993:2655–2665.
16. Miller TP, Grogan TM, Dalton WS, et al. P-glycoprotein expression in malignant lymphoma and reversal of clinical drug resistance with chemotherapy plus high dose verapamil. *J Clin Oncol* 1991;9:17–24.
17. Goldstein LJ, Galski H, Fojo A, et al. Expression of a multidrug resistance gene in human cancers. *J Natl Cancer Inst* 1989;81:116–124.
18. Liotta LA, Stetler-Stevenson WG. Principles of molecular cell biology of cancer: cancer metastasis. In: DeVita VT, Hellman S, Rosenberg SA, eds. *Cancer, principles and practice of oncology*, 4th ed. Philadelphia: J.B. Lippincott; 1993:340–348.
19. Dimitrakopoulou-Strauss A, Strauss LG, Goldschmidt H, et al. Evaluation of tumor metabolism and multidrug resistance in patients with malignant lymphomas. *Eur J Nucl Med* 1995;22:434–442.
20. Israel O, Front D, Lam M, et al. Gallium-67 imaging in monitoring lymphoma response to treatment. *Cancer* 1988;61:2439–2443.
21. Wylie BR, Southee AE, Joshua DE, et al. Gallium scanning in the management of mediastinal Hodgkin's disease. *Eur J Haematol* 1989;42:344–347.
22. Gasparini MD, Balzarini L, Castellani M, et al. Current role of gallium scan management of mediastinal Hodgkin lymphoma. *Cancer* 1993;72:577–582.
23. Lin J, Leung W, Ho SKW, et al. Quantitative evaluation of thallium-201 uptake in predicting chemotherapeutic response of osteosarcoma. *Eur J Nucl Med* 1995;22:553–555.

Scintigraphy of Posterior Tibial Tendinitis

David Groshar, Aharon Liberson, Michael Alperson, David G. Mendes, Michael Rozenbaum and Itzhak Rosner
Departments of Nuclear Medicine, Orthopedics and Rheumatology, Bnai Zion Medical Center; and the Faculty of Medicine, Technion-Institute of Technology, Haifa, Israel

Our goal was to describe the typical scintigraphic pattern of posterior tibial tendinitis. **Methods:** Bone scintigraphs were reviewed to study the scintigraphic characteristics of posterior tibial tendinitis in nine patients with posterior tibial tendinitis related to generalized rheumatic disease and in eight patients with isolated posterior tibial tendinitis. **Results:** The scintigraphic pattern of posterior tibial tendinitis is elongated increased uptake in the blood flow and blood-pool phase along the anatomical course of the tibialis posterior tendon at the medial aspect of the ankle (malleolus region). Static images demonstrate increased focal abnormal uptake at the medial malleolus and in the navicular bone. **Conclusion:** Bone scintigraphy depicts a characteristic pattern of posterior tibial tendinitis. It is useful for the early diagnosis of idiopathic- or rheumatic-related posterior tibial tendinitis.

Key Words: posterior tibial tendinitis; bone scintigraphy

J Nucl Med 1997; 38:247–249

Tendinitis due to an inflammatory process, degenerative change, endocrine and metabolic disorder or trauma initiates a periosteal reaction with reactive new bone formation at the entheses (*1,2*). This will result in an increased uptake of ^{99m}Tc-MDP caused by the increased bone turnover at the site of tendon attachment. Recently, it has been recognized that inflammatory changes of the tibialis posterior tendon occur more frequently than previously believed (*3,4*). Bone scintigraphy is used to detect areas of abnormal bone turnover in various musculoskeletal diseases (*1,5,6*). The bone scintigraphic pattern in enthesopathies at the calcaneus (plantar fasciitis and achilles tendinitis), tibial tuberosity (patellar tendinitis), greater trochanter, inferior pubic ramus and anterior inferior iliac spine has been reported (*7–12*). However, the pattern of posterior tibial tendinitis is not yet recognized. The purpose of this study was to describe the scintigraphic characteristic findings of posterior tibial tendinitis.

Received Jan. 12, 1996; revision accepted Apr. 17, 1996.
For correspondence or reprints contact: David Groshar, MD, Department of Nuclear Medicine, Bnai Zion Medical Center, POB 4940, Haifa, Israel 31048.

MATERIALS AND METHODS

Seventeen patients with posterior tibial tendinitis were studied. Three men and five women, aged 30–68 yr, had idiopathic posterior tibial tendinitis and in five men and four women, aged 21–75 yr, posterior tibial tendinitis was associated with systemic inflammatory disease (two rheumatoid arthritis, two undifferentiated spondyloarthropathy, one fibromyalgia, one reactive arthritis, one psoriasis arthritis, one pseudogout and one patient with gout and pseudogout). Diagnosis of posterior tibial tendinitis was based on clinical signs and symptoms which include pain, swelling and tenderness on palpation of the tendon, presence of low or flat longitudinal arch (pes planus deformity) and weakness during inversion of the foot. In the idiopathic posterior tibial tendinitis patients, the duration of symptoms was 3–48 mo. Response was achieved with systemic anti-inflammatory treatment in five patients and with systemic and local anti-inflammatory treatment in one. Two patients did not respond to systemic or local anti-inflammatory treatment and underwent surgery, and tenosynovitis was confirmed on histology. MRI diagnosis of posterior tibial tendinitis was obtained in two patients. In the posterior tibial tendinitis associated with systemic inflammatory disease, the duration of symptoms was 4–12 mo with response to systemic anti-inflammatory treatment.

Bone scintigraphy was performed after intravenous injection of 20–25 mCi ^{99m}Tc-MDP. A digital gamma camera with an all-purpose, low-energy collimator was used. A blood flow study was obtained in the anterior or plantar view of the feet with dynamic acquisition of 1 frame/2 sec for 32 sec. Immediate blood-pool and delayed (2–4-hr) planar scans of the feet in the anterior, medial, lateral and plantar views were obtained using static acquisition with 400,000 counts.

RESULTS

The scintigraphic pattern of posterior tibial tendinitis found in all patients was an elongated increased uptake in the blood-flow (Fig. 1) and blood-pool phase (Fig. 2) of the study in the anatomical course of the tibialis posterior tendon at the medial malleolus region. The delayed static images demonstrated